BIMA ARRAY DETECTIONS OF HCN IN COMETS LINEAR (C/2002 T7) AND NEAT (C/2001 Q4)

D. N. Friedel[1], Anthony J. Remijan[2,3], L. E. Snyder[1], M. F. A'Hearn[4], Geoffrey A. Blake[5], Imke de Pater[6], H. R. Dickel[1], J. R. Forster[6], M. R. Hogerheijde[7], C. Kraybill[6], L. W. Looney[1], Patrick Palmer[8], & M. C. H. Wright[6]

ABSTRACT

We present interferometric detections of HCN in comets LINEAR (C/2002 T7) and NEAT (C/2001 Q4) with the Berkeley-Illinois-Maryland Association (BIMA) Array. With a $25''.4 \times 20''.3$ synthesized beam around Comet LINEAR and using a variable temperature and outflow velocity (VTOV) model, we found an HCN column density of $< N_T >= 6.4 \pm 2.1 \times 10^{12}$ cm^{-2}, and a production rate of Q(HCN)=$6.5 \pm 2.2 \times 10^{26}$ s^{-1}, giving a production rate ratio of HCN relative to H_2O of $\sim 3.3 \pm 1.1 \times 10^{-3}$ and relative to CN of $\sim 4.6 \pm 1.5$. With a $21''.3 \times 17''.5$ synthesized beam around Comet NEAT and using a VTOV model, we found an HCN column density of $< N_T >= 8.5 \pm 4.5 \times 10^{11}$ cm^{-2}, and a

[1]Department of Astronomy, 1002 W. Green St., University of Illinois, Urbana IL 61801
email: friedel@astro.uiuc.edu, snyder@astro.uiuc.edu, lwl@astro.uiuc.edu, lanie@astro.uiuc.edu

[2]NASA Goddard Space Flight Center, Computational and Information Sciences and Technologies Office, Code 606 , Greenbelt, MD 20771
email: aremijan@pop900.gsfc.nasa.gov

[3]National Research Council Resident Research Associate

[4]Department of Astronomy, University of Maryland, College Park MD 20742-2421
email: ma@astro.umd.edu

[5]Division of Geological and Planetary Sciences; Division of Chemistry and Chemical Engineering California Institute of Technology 150-21, Pasadena, CA 91125
email: gab@gps.caltech.edu

[6]Department of Astronomy, University of California, Berkeley, CA 94720
email: imke@floris.berkeley.edu, rforster@astro.berkeley.edu, ckraybill@astro.berkeley.edu, wright@astro.berkeley.edu

[7]Leiden Observatory, PO Box 9513, 2300 RA, Leiden, The Netherlands
email: michiel@strw.leidenuniv.nl

[8]Department of Astronomy and Astrophysics, University of Chicago, Chicago, IL 60637
email: ppalmer@oskar.uchicago.edu

production rate of Q(HCN)=$8.9 \pm 4.7 \times 10^{25}$ s^{-1}, giving a production rate ratio of HCN relative to H_2O of $\sim 7.4 \pm 3.9 \times 10^{-4}$ and relative to CN of $\sim 0.3 \pm 0.2$. For both comets, the production rates relative to H_2O are similar to those found in previous comet observations. For Comet LINEAR the production rate relative to CN is consistent with HCN being the primary parent species of CN, while for Comet NEAT it is too low for this to be the case.

Subject headings: comets: individual (LINEAR (C/2002 T7), NEAT (C/2001 Q4)) - molecular processes - techniques: interferometric - radio lines: solar system

1. INTRODUCTION

HCN has been extensively studied around several comets including Comet P/Halley (Despois et al. 1986), Comet Hyakutake (C/1996 B2) (e.g., Mumma et al. 1996; Lis et al. 1997; Womack, Festou, & Stern 1997; Biver et al. 1999a), Comet Hale-Bopp (C/1995 O1) (e.g., Fitzsimmons & Cartwright 1996; Wright et al 1998; Hirota et al. 1999; Irvine et al. 1999; Magee-Sauer et al. 1999; Ziurys et al. 1999; Veal et al. 2000; Snyder et al. 2001; Woodney et al. 2002) and Comet LINEAR (C/1999 S4) (Bockelée-Morvan et al. 2001; Hogerheijde et al. 2004). Veal et al. (2000) made some of the first interferometric observations of HCN in Comet Hale-Bopp. From the distribution and temporal behavior of the HCN emission, they were able to make very accurate calculations of the HCN production rate as well as modeling its distribution in the coma using a spherical Haser model (Haser 1957). The deviations from the Haser model were explained by the existence of jets releasing HCN gas, a conclusion directly supported by high spatial resolution interferometric imaging of Comet Hale-Bopp by Blake et al. (1999). Snyder et al. (2001) followed up the observations of Veal et al. (2000) and found the measured HCN scale length to be very similar to the theoretical predictions of Huebner, Keady, & Lyon (1992a) and Crovisier (1994).

In the Spring of 2004, we were awarded a rare opportunity to observe two comets passing into the inner solar system and within ~0.3 AU of the Earth. Comet LINEAR (C/2002 T7) reached perigee on 2004 May 19, coming within 0.27 AU, while Comet NEAT (C/2001 Q4) reached perigee on 2004 May 7, coming within 0.32 AU. Both comets were identified as being dynamically new; such comets reach a peak of strong activity as they approach perihelion. It was extremely important to observe both comets when they were close to both perihelion and perigee in order to observe them near their peak emission and their maximum signal due to their proximity.

This paper describes the results of an effort to observe HCN in both Comets LINEAR and NEAT, with the Berkeley-Illinois-Maryland Association (BIMA) Array[9] near Hat Creek, California (§2). We present interferometric detections of HCN in both comets and calculate the total beam averaged HCN column densities and production rates by two methods. The first assumes the realistic scenario of a temperature and outflow velocity that vary with cometocentric distance and the second model assumes a constant temperature and outflow velocity throughout the coma.

2. OBSERVATIONS

We used the BIMA Array at Hat Creek, California ($122^o28'8''.4$ West, $40^o49'2''.28$ North; altitude 1333 m) in D-configuration (baselines from ∼6m to ∼35m) cross-correlation mode to observe HCN in Comets LINEAR (C/2002 T7) and NEAT (C/2001 Q4) during their 2004 apparitions.

The HCN observations of Comet LINEAR, using JPL reference orbit 69, were taken 2004 May 11 toward the topocentric coordinates α=$01^h15^m59.^s06$; δ=$-07^o39'16.5''$ [J2000.0][10] at the beginning of our observations (16:54 UT), and moved to α=$01^h18^m20.^s56$; δ=$-07^o52'33.9''$ [J2000.0] by the end of our observations (20:58 UT). The comet was at a heliocentric distance of 0.73 AU and a geocentric distance of 0.44 AU ($1''$=319 km at 0.44 AU). The spectral window containing the HCN hyperfine components had a bandwidth of 50 MHz and was divided into 128 channels giving a channel spacing of 0.39 MHz (1.321 km s^{-1}). W3(OH) was used as the flux density calibrator for this observation. The quasar 0108+015 was used to calibrate the antenna based gains.

The HCN observations of Comet NEAT, using JPL reference orbit 123, were taken 2004 May 23 toward the topocentric coordinates α=$09^h13^m54.^s67$; δ=$36^o46'30.7''$ [J2000.0] at the beginning of our observations (20:58 UT), and moved to α=$09^h15^m23.^s16$; δ=$37^o18'34.9''$ [J2000.0] by the end of our observations (06:51 May 24 UT). The comet was at a heliocentric distance of 0.97 AU and a geocentric distance of 0.61 AU ($1''$=442 km at 0.61 AU). The spectral resolution was the same as for Comet LINEAR. Mars was used as the flux density calibrator and 0927+390 was used to calibrate the antenna based gains.

The absolute amplitude calibration is accurate to within ∼20%. We note that our

[9]Operated by the University of California, Berkeley, the University of Illinois, and the University of Maryland with support from the National Science Foundation.

[10]We believe the positional accuracy to be good to a few arcseconds for our observations. This error is insignificant relative to the size of the synthesized beams (see §3).

observations may cover a significant amount of the rotation period of Comets LINEAR and NEAT. However, to date no rotation period has been given for either comet, thus we are unable to comment on any effects this may have on our results. The data were combined and imaged using the MIRIAD software package (Sault, Teuben, & Wright 1995). Table 1 lists the HCN molecular line parameters. The HCN spectroscopic constants were taken from Maki (1974). In the following, our analysis is for the strongest component, the $J = 1 - 0$, $F = 2 - 1$ transition.

3. RESULTS

Figure 1(a-c) shows our map and spectra of HCN around Comet LINEAR (C/2002 T7). Figure 1a shows the map of the $J = 1 - 0, F = 2 - 1$ transition of HCN in 1 σ contours, starting at 2 σ. The synthesized beam of $25''.4 \times 20''.3$ is shown at the bottom left of the map. The line segment in the image shows the projection of the direction toward the sun. The origin of the line segment is anchored at the predicted position of the comet nucleus. The coordinates are given in offset arcseconds centered on the comet nucleus. We note that the peak intensity of the HCN emission is offset from the predicted position of the nucleus by $\sim 5''$ along the semi-major axis of the synthesized beam. In general, the positional uncertainty roughly scales as the beamsize/SNR. For Comet LINEAR this uncertainty is 4-5$''$, so the offset is not significant[11]. Figure 1b shows the cross-correlation spectrum of this transition. The dashed line corresponds to the rest frequency of the $J = 1 - 0, F = 2 - 1$ line for a cometocentric rest velocity of 0 km s^{-1}. The 1 σ rms noise level is seen at the left of the panel. The $F = 2 - 1$ line for Comet LINEAR was fit with a Gaussian by a least-squares method which gives a peak intensity of 0.59$\pm$0.14 Jy beam^{-1}, a FWHM of 1.38$\pm$0.34 km s^{-1}, and a cometocentric velocity of -0.29$\pm$0.28 km s^{-1}. Figure 1c shows the cross-correlation spectrum (Hanning smoothed over three channels) of this transition.

Figure 1(d-f) shows our map and spectra of HCN around Comet NEAT (C/2001 Q4). Figure 1d shows the map of the $J = 1 - 0, F = 2 - 1$ transition of HCN in 1 σ contours, starting at 2 σ. The synthesized beam of $21''.3 \times 17''.5$ is shown at the bottom left of the map. We note, as with Comet LINEAR, that the HCN peak intensity is offset by $\sim 5''$ along the semi-major axis of our synthesized beam and that there is also some elongation of the source along this axis. We consider neither the offset nor the elongation to be significant because these are most likely due to the beam size and the low SNR. Figure 1e shows the cross-correlation spectrum of this transition. The dashed line is similar to Figure 1b for a

[11]This does not include any uncertainties in the ephemeris.

cometocentric rest velocity of 0 km s^{-1}. The $F = 2 - 1$ line appears in only a single channel so we will assume a FWHM of ∼1.3 km s^{-1} for HCN. Figure 1f shows the cross-correlation spectrum (Hanning smoothed over three channels) of this transition.

4. DISCUSSION

4.1. Column Densities and Production Rates

In the innermost coma, collisions between cold cometary species dominate the rotational population of the gas, but in the less dense outer coma the collision time becomes longer than the time for absorption of solar photons and the subsequent cascade of emission In that case, the population can also be determined by solar radiation driven fluorescence. Fluorescence effects could allow LTE to be maintained at a lower density than required in optically thin cases (e.g., Crovisier et al. 1984; Bockelée-Morvan et al. 1987). Lovell et al. (2004) determined that for the $J = 1 - 0$ transition of HCN for Comet Hyakutake (C/1996 B2) the transition between collisionally dominated and fluorescence dominated emission is between 26,000 and 38,000 km from the nucleus. Since both Comet LINEAR and Comet NEAT have similar water production rates relative to Comet Hyakutake (D. G. Schleicher, 2004, private communication)(see §4.2) at comparable heliocentric distances, we assume their transition radii are also comparable. On the sky this translates to 82-119″ for Comet LINEAR and 59-86″ for Comet NEAT.

The synthesized beams sample a cylinder of gas through each comet[12], and because the HCN volume density falls off faster than r^{-2} due to photodissociation, most of the contribution to the integrated line intensity will come from a sample on the order of the size of the projected synthesized beam. Since the synthesized beam is much smaller than the outer radii of the collisionally dominated regions, conditions significantly outside of the beam are not likely to affect our observations.

The contribution from different cometocentric radii (i.e. from different source sizes) is determined by two factors. The first is that sources of differing size but equal total flux do not have equal peak fluxes and thus, when summed together, do not contribute equally to the total peak flux of a map. The second is that the array starts to resolve out flux from sources that are much larger than the synthesized beam. The first effect is dominant for

[12]In a small cylinder passing through the cometary gas, only a small fraction of the HCN will be in the less dense fluorescent zone. Hence, unlike the case for some optical molecular observations, here we assume that the HCN in the fluorescence zone can be ignored relative to that in the denser collisional zone.

source sizes that are on the order of the synthesized beam while the second becomes more dominant for larger source sizes. These two effects are illustrated in Figure 2. The top panel is from our Comet LINEAR observations and the lower panel is from our Comet NEAT observations. The abscissa is cometocentric radius in arcseconds of a source on the sky and the ordinate is r_i, the array recovery factor (see Appendix A for a detailed explanation). The collisionally dominated region of the coma is labeled "Collisional Zone", the transition between the collisionally dominated and fluorescence dominated regions is denoted by the hatching, and the fluorescence dominated region is labeled "Fluorescence Zone". The solid line shows the peak flux detected by the array from each source size as a percentage of the peak flux of a point source of equal total flux. Thus, both from this figure and the above argument, it is clear that we are sampling the collisionally dominated region and are insensitive to fluorescence effects.

Our calculations are made assuming optically thin emission, since the limits on the satellite hyperfine components show that they are significantly weaker than the main component. For cross-correlation observations, $< N_T >$, the beam-averaged molecular column density, is

$$< N_T >= \frac{2.04\ W_{\rm I}\ Z\ e^{E_{\rm u}/T_{\rm rot}}}{\theta_{\rm a}\theta_{\rm b} S\mu^2\nu^3} \times\ 10^{20}\ {\rm cm}^{-2}. \qquad (1)$$

In equation (1), $W_{\rm I} = \int I_\nu dv$ in Jy beam^{-1} km s^{-1}, and I_ν is the flux density per beam. Z is the rotational partition function ($Z = 0.47T_{\rm rot}$), E_u is the upper state energy of the transition, $T_{\rm rot}$ is the rotation temperature, $\theta_{\rm a}$ and $\theta_{\rm b}$ are the FWHM synthesized beam dimensions in arcsec, S is the line strength, μ the dipole moment in Debye, and ν is the frequency in GHz.

From the least squares fit to the Comet LINEAR spectrum, we find an integrated line intensity of 1.46±0.49 Jy beam^{-1} km s^{-1} for the $J = 1-0, F = 2-1$ HCN line around Comet LINEAR[13]. From Figure 1e, we find an integrated line intensity of 0.22±0.11 Jy beam^{-1} km s^{-1} for the $J = 1-0, F = 2-1$ HCN line around Comet NEAT[14].

4.1.1. Model 1: Assuming Variable Temperatures and Outflow Velocities

We consider the case where the temperature and outflow velocity vary with cometocentric distance, as has been observed and modeled in previous comets (e.g. Comet Hyakutake

[13]To convert this to integrated main beam brightness temperature multiply by 0.30 K/(Jy beam^{-1}).

[14]To convert this to integrated main beam brightness temperature multiply by 0.42 K/(Jy beam^{-1}).

and Comet Hale-Bopp (Combi et al. 1999a,b)). We label this as the variable temperature and outflow velocity (VTOV) model. In order to do this, we modeled the HCN emission as concentric shells (of thickness 100 km out to a radius of 10,000 km and a thickness of 2000 km for radii of 10,000-30,000 km) around the nucleus and calculated the total column density and production rate. Since we consider both comets to be similar to Comet Hyakutake, we used the velocity profiles from Figure 3 of Combi et al. (1999a) or the fit to that data from Lovell et al. (2004) to give velocities to each shell. The April 9 profile was used for Comet LINEAR and the March 30 profile and fit was used for Comet NEAT, since on these dates Comet Hyakutake was at a similar heliocentric distance. These velocities were scaled to match the observed velocity profile of the spectral line, taking into account thermal broadening. Similarly, the temperature profiles for each comet were also taken from Combi et al. (1999a). Our VTOV model is explained in detail in Appendix A, and gives total beam averaged column densities of $< N_T > = 6.4 \pm 2.1 \times 10^{12}$ cm^{-2} for Comet LINEAR and $< N_T > = 8.5 \pm 4.5 \times 10^{11}$ cm^{-2} for Comet NEAT and production rates of Q(HCN)=$6.5 \pm 2.2 \times 10^{26}$ s^{-1} for Comet LINEAR and Q(HCN)=$8.9 \pm 4.7 \times 10^{25}$ s^{-1} for Comet NEAT.

4.1.2. Model 2: Assuming Constant Temperatures and Outflow Velocities

In the case of assuming a constant T_{rot} the calculation of total beam averaged column density is straightforward, using equation (1). For Comet LINEAR we assume a rotation temperature of 115 K (DiSanti et al. 2004; Magee-Sauer et al. 2004; Küppers et al. 2004) and for Comet NEAT we assume a rotation temperature of 52 K. The temperature for Comet NEAT was derived from Figure 3 of Combi et al. (1999a) by averaging across the section of their March 30 curve we are sensitive to, when Comet Hyakutake was at a similar heliocentric distance. Using the above temperature for Comet LINEAR we find a total beam averaged HCN column density (corrected for the other hyperfine components) of $< N_T > = 9.5 \pm 3.2 \times 10^{12}$ cm^{-2}. Using the above temperature for Comet NEAT we find a total beam averaged HCN column density (corrected for the other hyperfine components) of $< N_T > = 9.6 \pm 5.1 \times 10^{11}$ cm^{-2}.

To calculate Q_p, the parent molecule production rate, we use the total beam averaged column densities with the Haser model (Haser 1957). Since the Haser model assumes a constant outflow velocity, it is better suited for the fluorescence region rather than the inner, collisionally dominated, coma. However, we will compare the Haser model results with our model since the Haser model has been commonly used by previous cometary observations (Hogerheijde et al. 2004; Snyder et al. 2001; Veal et al. 2000; Wright et al 1998).

For a photodissociation scale length λ_p, nuclear radius r_n, and constant radial outflow velocity v_0, the density as a function of r, $n_p(r)$, is given by Snyder et al. (2001):

$$n_p(r) = \frac{Q_p}{4\pi r^2 v_0} e^{-\frac{(r-r_n)}{\lambda_p}}. \tag{2}$$

For Comets LINEAR and NEAT, we assume a nuclear radius of $r_n = 5$ km. We use a radial outflow velocity of $v_0 = 0.62$ km s^{-1} for Comet LINEAR, based on the HWHM of the Gaussian fit and taking into account the 10% increase in line width due to thermal broadening (Biver et al. 1999b) and $v_0 = 0.59$ km s^{-1} for Comet NEAT, based on the single channel half width of the line and taking into account thermal broadening.

Consider a point on the line of sight that passes a projected distance, p, in the plane of the sky from the nucleus. For a given value of z, measured along the line of sight, this will correspond to a radial distance $r = \sqrt{(p^2 + z^2)}$ from the nucleus. The column density, N_p, is given by Snyder et al. (2001):

$$N_p(p) = \frac{Q_p}{4\pi v_0} e^{\frac{r_n}{\lambda_p}} \int_{-\infty}^{\infty} \frac{\exp\{-[(p^2 + z^2)^{1/2}/\lambda_p]\}}{(p^2 + z^2)} dz. \tag{3}$$

Finally, N_p from equation (3) may be averaged over the synthesized beam and equated to $< N_T >$, the beam-averaged molecular column density, in order to obtain Q_p, the parent molecule production rate from the Haser model.

The Quiet Sun HCN photodissociation rate in the Solar UV field at $r_{hel} = 1$ AU is given by Huebner et al. (1992a) as $\alpha(1 \text{ AU}) = 1.3 \times 10^{-5}$ s^{-1} and by Crovisier (1994) as 1.5×10^{-5} s^{-1}. The expected accuracy is 10-20% (Crovisier 1994), so this is reasonable agreement. Thus we will assume α(1 AU)=1.3×10^{-5} s^{-1} (equivalent to $\sim 3.7 \times 10^4$ km for Comet NEAT and $\sim 2.2 \times 10^4$ km for Comet LINEAR). We find that the May 11 data around Comet LINEAR give a production rate, Q(HCN), of $5.1 \pm 1.7 \times 10^{26}$ s^{-1}, and the May 23 data around Comet NEAT give a production rate of $5.7 \pm 3.0 \times 10^{25}$ s^{-1}.

4.1.3. Comparison of Models

The column densities calculated with the VTOV model (model 1) are 11-33% lower than those calculated with model 2. However, the production rates calculated with the VTOV model are 22-36% higher than those calculated with the Haser model (see model 2 in §4.1.2). These differences are not large. However, the VTOV model provides a better approximation than the Haser model for the physical conditions in the cometary collisional regions that the BIMA Array sampled. Consequently, for the interferometric observations discussed in this paper, the VTOV model should produce more realistic results than the Haser model.

Table 2 gives a comparison of the two methods. Column 1 gives the comet name, column 2 gives the total column density, column 3 gives the production rate, column 4 gives the HCN/H_2O ratio (see §4.2) and column 5 gives the HCN/CN ratio (see §4.3).

4.2. Relative Production Rates of HCN to H_2O

4.2.1. Comet NEAT

D. G. Schleicher (2005, private communication) measured H_2O production rates from Comet NEAT and derived a scaling law of $Q(H_2O) \sim r_H^{-4.3}$, where r_H is the heliocentric distance of the comet. From his observations in May and June of 2004 and the scaling law, we scaled the H_2O production rates from the heliocentric distances when they were measured to 0.97 AU for Comet NEAT to match the r_H of our observations. Table 3 gives the measurements and their scaled values. Column 1 gives the date of observation, column 2 gives the heliocentric distance of the comet, columns 3 and 4 give the measured production rates of H_2O and CN (see §4.3), and columns 5 and 6 give the scaled production rates for H_2O and CN, respectively. The average value for Comet NEAT is Q(H_2O)$\sim 1.2 \times 10^{29}$ s^{-1}, which is very similar to water production rates measured from Comet Hyakutake at similar heliocentric distances to our observations ($\sim 1 \times 10^{29}$ s^{-1} (Lis et al. 1997)). If we assume a constant temperature and outflow velocity we find the production rate of HCN relative to H_2O for Comet NEAT is $\sim 4.7 \pm 2.5 \times 10^{-4}$. On the other hand, if we assume the more realistic VTOV model, we find the production rate of HCN relative to H_2O to be $\sim 7.4 \pm 3.9 \times 10^{-4}$ for Comet NEAT. This is similar to the ratios observed around previous comets such as Comet Hyakutake (1×10^{-3}) (Lis et al. 1997).

4.2.2. Comet LINEAR

H_2O production rates were also measured for Comet LINEAR by D. G. Schleicher (2005, private communication). From his data, he estimated the H_2O production rate to be $\sim 2 \times 10^{29}$ s^{-1} during our May 11 observations. If we assume a constant temperature and outflow velocity, we find the production rate of HCN relative to H_2O is $\sim 2.6 \pm 0.9 \times 10^{-3}$ for Comet LINEAR. On the other hand, if we assume the more realistic VTOV model, we find the production rate of HCN relative to H_2O to be $\sim 3.3 \pm 1.1 \times 10^{-3}$. This is similar to the ratio observed around Comet Hale-Bopp ($2.1 - 2.6 \times 10^{-3}$) (Snyder et al. 2001).

4.3. Relative Production Rates of HCN to CN

4.3.1. Comet NEAT

D. G. Schleicher (2005, private communication) measured CN production rates from Comet NEAT and derived a scaling law of $Q(CN) \sim r_H^{-2.1}$. From his observations in May and June 2004 and the scaling law, we scaled these values from the heliocentric distances when they were measured to the heliocentric distance of Comet NEAT during our observations (see Table 3). Averaging these values gives Q(CN) $\sim 2.6 \times 10^{26}$ s^{-1} for Comet NEAT. If we assume a constant temperature and outflow velocity we find the production rate of HCN relative to CN is $\sim 0.2 \pm 0.1$ for Comet NEAT. On the other hand, if we assume the more realistic VTOV model, we find the production rate of HCN relative to CN of $\sim 0.3 \pm 0.2$ for Comet NEAT. The photodissociative branching ratio of HCN implies that ∼97% of HCN will be photodissociated into H and CN (Huebner, Keady, & Lyon 1992b). Woodney et al. (2002) concluded that HCN is most likely the primary parent species of CN. Thus, one would expect the HCN to CN ratio to be near 1. However, the ratio for Comet NEAT is a factor of ∼3 smaller than the expected ratio.

4.3.2. Comet LINEAR

CN production rates were measured for Comet LINEAR by D. G. Schleicher (2005, private communication). From his data, he estimated the CN production rate to be $\sim 1.4 \times 10^{26}$ s^{-1} during our May 11 observations. If we assume a constant temperature and outflow velocity we find the production rate of HCN relative to CN is $\sim 3.6 \pm 1.2$ for Comet LINEAR. On the other hand, if we assume the more realistic VTOV model, we find the production rate of HCN relative to CN to be $\sim 4.6 \pm 1.5$.

5. SUMMARY

We have detected the $J = 1 - 0$ transition of HCN in Comets NEAT (C/2001 Q4) and LINEAR (C/2002 T7). We have calculated the total column density and production rates by two different models. The first (VTOV) model assumes the realistic scenario of temperature and outflow velocity that vary with cometocentric distance. We compare this model to one where the temperature and outflow velocity are constant throughout the coma (Haser model). The differences between the outcomes of the models are ∼11-33% for N_T and ∼22-36% for Q. However, for the interferometric observations described in this paper, more realistic results will be obtained by using the VTOV model outlined in Sec. 4.1.1 and Appendix A. This model gives production rates of Q(HCN)=$6.5 \pm 2.2 \times 10^{26}$ s^{-1} and ratios of HCN/H_2O and HCN/CN of $\sim 3.3 \pm 1.1 \times 10^{-3}$ and $\sim 4.6 \pm 1.5$, respectively, for Comet LINEAR and Q(HCN)=$8.9 \pm 4.7 \times 10^{25}$ s^{-1} and ratios of HCN/H_2O and HCN/CN of $\sim 7.4 \pm 3.9 \times 10^{-4}$ and $\sim 0.3 \pm 0.2$, respectively, for Comet NEAT.

The HCN production rate relative to H_2O for Comet NEAT is similar to that found previously for Comet Hyakutake (Lis et al. 1997), while the ratio for Comet LINEAR is similar to that observed from the highly productive Comet Hale-Bopp (Snyder et al. 2001). The HCN production rate relative to CN for Comet LINEAR is consistent with HCN being the primary parent of CN, as was suggested in Woodney et al. (2002). However, for Comet NEAT the value is too low.

We thank J. R. Dickel for assisting with the observations, an anonymous referee for many helpful comments, and D. G. Schleicher for providing H_2O and CN production rates. This work was partially funded by: NSF AST02-28953, AST02-28963, AST02-28974 and AST02-28955; and the Universities of Illinois, Maryland, and California, Berkeley.

APPENDIX

A. DESCRIPTION OF THE VTOV MODEL

The variable temperature and outflow velocity (VTOV) model consists of concentric spherical shells centered on a cometary nucleus of radius 5 km. The shells had a thickness of 100 km (with the exception of the 1st shell (95 km)) out to a cometocentric radius of 10,000 km and a thickness of 2,000 km for radii from 10,000 to 30,000 km. 30,000 km is equivalent to a cometocentric radius of 94″on the sky for Comet LINEAR and 67.9″for Comet NEAT. This distance was chosen as the outer limit of our model because the structures of this size contribute less than 0.1% to the peak flux and the population of HCN at this radius is less than 40% that of the central shell due to photodissociation. Thus, by the combination of these factors the contribution from any shells beyond 30,000 km would be negligible.

While quantities such as the outflow velocity and temperature vary in a very non-linear way across the coma of each comet, the changes across any given shell are small enough to be considered linear. Thus, the quantities calculated for each shell, unless otherwise specified, are calculated at the average radius of each shell, since they will be very close to the average value for the entire shell.

For the model we calculate the following quantities for each shell i in our model :

1. The time, t_i, each molecule spends in the shell, is given by

$$t_i = \frac{(R_i - R_{i-1})}{V_i}, \tag{A1}$$

   where R_i and R_{i-1} are the outer and inner radii of shell i, respectively, and V_i is the average velocity of the molecule across the shell (from Combi et al. (1999a)).

2. The total time, $t_{i,\mathrm{tot}}$, it takes a molecule to travel from the nucleus to the center of the shell, is given by

$$t_{i,\mathrm{tot}} = \left(\sum_{j=1}^{i-1} t_j\right) + \frac{t_i}{2}. \tag{A2}$$

3. The number of molecules, n_i, in each shell, is given by

$$n_i = Q t_i e^{-\alpha t_{i,\mathrm{tot}}/r_H^2}, \tag{A3}$$

   where Q is the production rate, α is the photodissociation rate (assumed to be α(1 AU)=1.3×10^{-5} s^{-1}), and r_h is the heliocentric radius of the comet. *Note*: At this point it does not matter what value we give Q since it does not vary from shell to shell and thus is a constant for this part of the model.

4. The BIMA Array's flux recovery factor for the projected size of the shell on the sky is defined as the peak flux of a shell compared to that of a point source. This is a combination of a geometric effect (i.e. the flux is spread out over larger areas for larger shells), which is dominant for source sizes comparable to our synthesized beam size, and the fact that the array resolves out flux from sources that are much larger than the synthesized beam (array filtering effect). The recovery factor is found in the following way:

   (a) Each source size (or shell) is modeled by first creating a Gaussian[15] source image for each concentric shell, of the appropriate FWHM and at the position on the sky of the comet, with the MIRIAD task IMGEN[16]. Every Gaussian shell is assumed to contribute equally to the flux recovery for a uniformly extended source.

---

[15] In this step we approximate the shells as Gaussian sources rather than as actual shells because any structure on the sky that has sharp edges, such as a shell, will produce ringing in the $u - v$ plane and artifacts in the final map. Since the actual observations of the comets observed continuous distributions on the sky with no sharp edges, approximating the shell by a Gaussian is reasonable.

[16] Detailed descriptions of all MIRIAD tasks can be found at: http://bima.astro.umd.edu/miriad/ref.html

(b) In order to remove geometric and filtering effects each image is run through UVMODEL to produce a $u - v$ data set that is the array's response to the input source based on the $u - v$ tracks of our actual observations.

(c) Each data set is then INVERTed, CLEANed, and RESTORed as normal to produce the final output map.

(d) The peak intensity (p_i) of each map is compared to that of a point source ($p_{\rm ps}$) model of equal integrated intensity to give the array's recovery factor, r_i, where,

$$r_i = \frac{p_i}{p_{\rm ps}}. \tag{A4}$$

Note that $r_i \rightarrow 0$ for an infinitely extended source, $r_i \rightarrow 1$ for a point source, and $r_i = 0.5$ if the source just fills the beam.

The array's recovery factor is illustrated in Figure 2. The top panel is for Comet LINEAR and the bottom panel is for Comet NEAT. The abscissa is cometocentric radius and the ordinate is r_i. The solid line shows r_i for all shells.

5. The production rate Q of the comet is found by modifying equation (1),

$$\frac{4ln(2)n_i r_i}{\pi ab} =< N_i >= \frac{2.04 W_i Z_i e^{E_u/T_i}}{\theta_{\rm a}\theta_{\rm b} S \mu^2 \nu^3} \times 10^{20} {\rm cm}^{-2}. \tag{A5}$$

We note that $4ln(2)/\pi ab$ is the projected area on the sky of our Gaussian synthesized beam (in cm^2), N_i is the beam averaged column density of the shell, W_i is the integrated line intensity of the shell, and T_i is the rotation temperature for the shell (from Combi et al. (1999a)). Rearranging equation (A5) and incorporating the fact that

$$W = \sum_i W_i \tag{A6}$$

gives

$$W = \frac{1.36\theta_a\theta_b S\mu^2\nu^3}{\pi ab} \sum_i \frac{n_i r_i}{Z_i e^{E_u/T_i}} \times 10^{-20}. \tag{A7}$$

Incorporating equation (A3) and rearranging equation (A7) gives

$$Q = \frac{0.736 W \pi ab}{\theta_a\theta_b S\mu^2\nu^3} \left(\sum_i \frac{r_i t_i e^{-\alpha t_{i,{\rm tot}}/r_H^2}}{Z_i e^{E_u/T_i}} \right)^{-1} \times 10^{20}. \tag{A8}$$

Since all factors on the right hand side of equation (A8) are known, Q can be found. *Note*: In equation (A5) we divided n_i by the projected beam area rather than the projected area of the shell, even for those shells with a projected area larger than our beam. This is done because, even though there are some molecules outside of the synthesized beam, they are contributing flux to the area inside the synthesized beam.

6. Now that Q has been found, use it in equation (A3) to find n_i. Then use each n_i in equation (A5) to find N_i for each shell. Then the total beam averaged column density, $< N_T >$, is given by the sum over all shells,

$$< N_T >= \sum_i < N_i > . \tag{A9}$$

REFERENCES

Biver, N., et al. 1999a, AJ, 118, 1850

Biver, N., et al. 1999b, Earth Moon and Planets, 78, 5

Blake, G. A., Qi, C., Hogerheijde, M. R., Gurwell, H. A., & Muhleman, D. O. 1999, Nature, 398, 213

Bockelée-Morvan, D., Crovisier, J., Despois, D., Forveille, T., Gerard, E., Schraml, J., & Thum, C. 1987, A&A, 180, 253

Bockelée-Morvan, et al. 2001, Science, 292, 1339

Combi, M. R., Cochran, A. L., Cochran, W. D., Lambert, D. L., & Johns-Krull, C. M. 1999, ApJ, 512, 961

Combi, M. R., Kabin, K., DeZeeuw, D. L., Gombosi, T. I., & Powell, K. G. 1999, Earth Moon and Planets, 79, 275

Crovisier, J. 1984, A&A, 130, 361

Crovisier, J. 1994, J. Geophys. Res., 99, 3777

Despois, D., Crovisier, J., Bockelee-Morvan, D., Gerard, E., & Schraml, J. 1986, A&A, 160, L11

DiSanti, M. A., Reuter, D. C., Mumma, M. J., Dello Russo, N., Magee-Sauer, K., Gibb, E. L., Bonev, B., & Anderson, W. M. 2004, AAS/Division for Planetary Sciences Meeting Abstracts, 36, 25.08

Fitzsimmons, A. & Cartwright, I. M. 1996, MNRAS, 278, L37

Haser, L. 1957, Academie royale de Belgique, Bulletin de la classe des Sciences, Ser 5, 43, 740

Hirota, T., Yamamoto, S., Kawaguchi, K., Sakamoto, A., & Ukita, N. 1999, ApJ, 520, 895

Hogerheijde, M. R., et al. 2004, AJ, 127, 2406

Huebner, W. F., Keady, J. J., & Lyon, S. P. 1992a, Ap&SS, 195, 291

Huebner, W. F., Keady, J. J., & Lyon, S. P. 1992b, Ap&SS, 195, 7

Irvine, W. M., Dickens, J. E., Lovell, A. J., Schloerb, F. P., Senay, M., Bergin, E. A., Jewitt, D., & Matthews, H. E. 1999, Earth Moon and Planets, 78, 29

Küppers, M., Hartogh, P., & Villanueva, G. 2004, AAS/Division for Planetary Sciences Meeting Abstracts, 36, 25.05

Lis, D. C., et al. 1997, Icarus, 130, 355

Lovell, A. J., Kallivayalil, N., Schloerb, F. P., Combi, M. R., Hansen, K. C., & Gombosi, T. I. 2004, ApJ, 613, 615

Magee-Sauer, K., Mumma, M. J., DiSanti, M. A., Russo, N. D., & Rettig, T. W. 1999, Icarus, 142, 498

Magee-Sauer, K., Dello Russo, N., DiSanti, M. A., Bonev, B., Gibb, E. L., & Mumma, M. J. 2004, AAS/Division for Planetary Sciences Meeting Abstracts, 36, 25.03

Maki, A. G. 1974, J. Phys. Chem. Ref. Data, 3, 221

Mumma, M. J., Disanti, M. A., dello Russo, N., Fomenkova, M., Magee-Sauer, K., Kaminski, C. D., & Xie, D. X. 1996, Science, 272, 1310

Sault, R. J., Teuben, P. J., & Wright, M.C.H. 1995, in: Astronomical Data Analysis Software and Systems IV, ASP Conference Series 77, ed. R.A. Shaw, H.E. Payne, & J.J.E. Hayes, 433

Snyder, L. E., et al. 2001, AJ, 121, 1147

Veal, J. M., et al. 2000, AJ, 119, 1498

Womack, M., Festou, M. C., & Stern, S. A. 1997, AJ, 114, 2789

Woodney et al. 2002, Icarus, 157, 193

Wright, M. C. H., et al. 1998, AJ, 116, 3018

Ziurys, L. M., Savage, C., Brewster, M. A., Apponi, A. J., Pesch, T. C., & Wyckoff, S. 1999, ApJ, 527, L67

Table 1. HCN Molecular Line Parameters

Quantum Numbers	Frequency (MHz)	E_u (K)	$< S_{i,j}\mu^2 >$ (Debye^2)
$J = 1 - 0, F = 1 - 1$	88,630.4157(10)	4.3	3.0
$J = 1 - 0, F = 2 - 1$	88,631.8473(10)	4.3	4.9
$J = 1 - 0, F = 0 - 1$	88,633.9360(10)	4.3	1.0

Table 2. Comparison of Constant Temperature and Velocity Results with Variable Temperature and Outflow Velocity (VTOV) Results

Comet	$< N_T >$ (cm^{-2})	Q(HCN) (s^{-1})	$\frac{Q(HCN)}{Q(H_2O)}$	$\frac{Q(HCN)}{Q(CN)}$
Constant Temperature and Outflow Velocity (Haser model)				
LINEAR	$9.5 \pm 3.2 \times 10^{12}$	$5.1 \pm 1.7 \times 10^{26}$	$2.6 \pm 0.9 \times 10^{-3}$	3.6 ± 1.2
NEAT	$9.6 \pm 5.1 \times 10^{11}$	$5.7 \pm 3.0 \times 10^{25}$	$4.7 \pm 2.5 \times 10^{-4}$	0.2 ± 0.1
Variable Temperature and Outflow Velocity (VTOV model)				
LINEAR	$6.4 \pm 2.1 \times 10^{12}$	$6.5 \pm 2.2 \times 10^{26}$	$3.3 \pm 1.1 \times 10^{-3}$	4.6 ± 1.5
NEAT	$8.5 \pm 4.5 \times 10^{11}$	$8.9 \pm 4.7 \times 10^{25}$	$7.4 \pm 3.9 \times 10^{-4}$	0.3 ± 0.2

Table 3. Scaling of H_2O and CN Production Rates From Comet NEAT[a]

Date	r_H (AU)	Q(H_2O) (s^{-1})	Q(CN) (s^{-1})	Scaled Q(H_2O)[b] (s^{-1})	Scaled Q(CN)[c] (s^{-1})
2004 May 11	0.97	1.3×10^{29}	2.6×10^{26}	1.3×10^{29}	2.6×10^{26}
2004 May 12	0.96	1.3×10^{29}	2.5×10^{26}	1.2×10^{29}	2.4×10^{26}
2004 June 09	1.05	8.9×10^{28}	2.4×10^{26}	1.3×10^{29}	2.8×10^{26}
2004 June 10	1.06	7.9×10^{28}	2.1×10^{26}	1.2×10^{29}	2.6×10^{26}

[a]Unscaled data from D. G. Schleicher(private communication).

[b]The H_2O production rates were scaled by $r_H^{-4.3}$ for each comet (see§4.2).

[c]The CN production rates were scaled by $r_H^{-2.1}$ for each comet (see§4.3).

Fig. 1.— Comet LINEAR (C/2002 T7) and NEAT (C/2001 Q4) single field HCN images and spectra. (a) Comet T7 emission contours from the $J = 1-0, F = 2-1$ transition of HCN at 88.6318 GHz. Contours indicate the HCN emission near its peak centered at a cometocentric velocity of 0 km/s. The contour levels are -0.226, 0.226, 0.339, 0.452, and 0.565 Jy/beam (1σ spacing). The peak is 0.63 Jy/beam. Image coordinates are arcseconds offsets relative to the predicted position of the nucleus. The synthesized beam of $25.41'' \times 20.34''$ is in the lower left and the line segment shows the solar direction. (b) HCN cross-correlation spectra. Abscissa is radial velocity relative to the comet nucleus. Ordinate is flux density per beam, I_ν, in Jy/beam; $\sigma \sim 0.113$ Jy/beam (indicated by the vertical bar at the left). The dashed line is centered on the rest frequency (88.6318 GHz).(c) HCN cross-correlation spectra (Hanning smoothed over 3 channels), labels the same as in (b). (d) Comet Q4 emission contours from the $J = 1-0, F = 2-1$ transition of HCN. Contours indicate the HCN emission near its peak centered at a cometocentric velocity of 0 km/s. The contour levels are -0.06, 0.06, 0.09, 0.12 and 0.15 Jy/beam (1σ spacing). The peak is 0.17 Jy/beam. Image coordinates are the same as in (a). The synthesized beam of $21.27'' \times 17.53''$ is in the lower left and the line segment shows the solar direction. (e) HCN cross-correlation spectra, abscissa and ordinate are the same as in (b); $\sigma \sim 0.03$ Jy/beam (indicated by the vertical bar at the left). The dashed line is centered on the rest frequency (88.6318 GHz). (f) HCN cross-correlation spectra (Hanning smoothed over 3 channels), abscissa and ordinate are the same as in (b).

Fig. 2.— BIMA Array response to source size for each comet. The upper panel is from our Comet LINEAR observations and the lower panel is from our Comet NEAT observations. The abscissa is cometocentric distance in arcseconds and the ordinate is the array recovery factor r_i. The region of the cometary coma that is dominated by collisions is labeled "Collisional Zone". The hatched area denotes the region where the transition between collisionally dominated and fluorescence dominated regions is. The region of the coma that is dominated by fluorescence is labeled "Fluorescence Zone". The solid line shows r_i for each source size. The Array response to different source sizes shows that we are sampling the inner, collisionally dominated region of the coma.

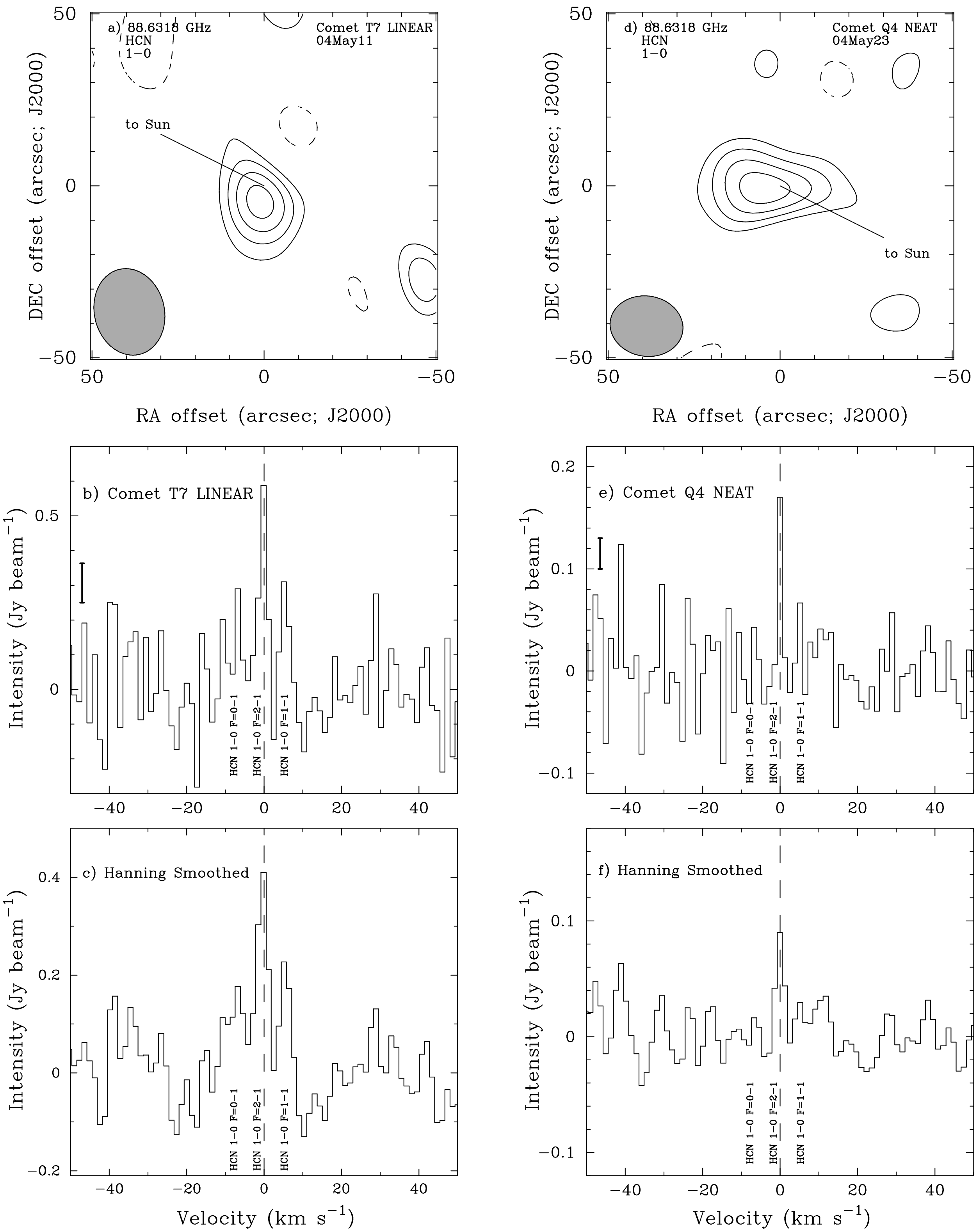
a) 88.6318 GHz
HCN
1–0
Comet T7 LINEAR
04May11
to Sun
d) 88.6318 GHz
HCN
1–0
Comet Q4 NEAT
04May23
to Sun
DEC offset (arcsec; J2000)
RA offset (arcsec; J2000)
b) Comet T7 LINEAR
e) Comet Q4 NEAT
c) Hanning Smoothed
f) Hanning Smoothed
HCN 1–0 F=0–1
HCN 1–0 F=2–1
HCN 1–0 F=1–1
Intensity (Jy beam^{-1})
Velocity (km s^{-1})

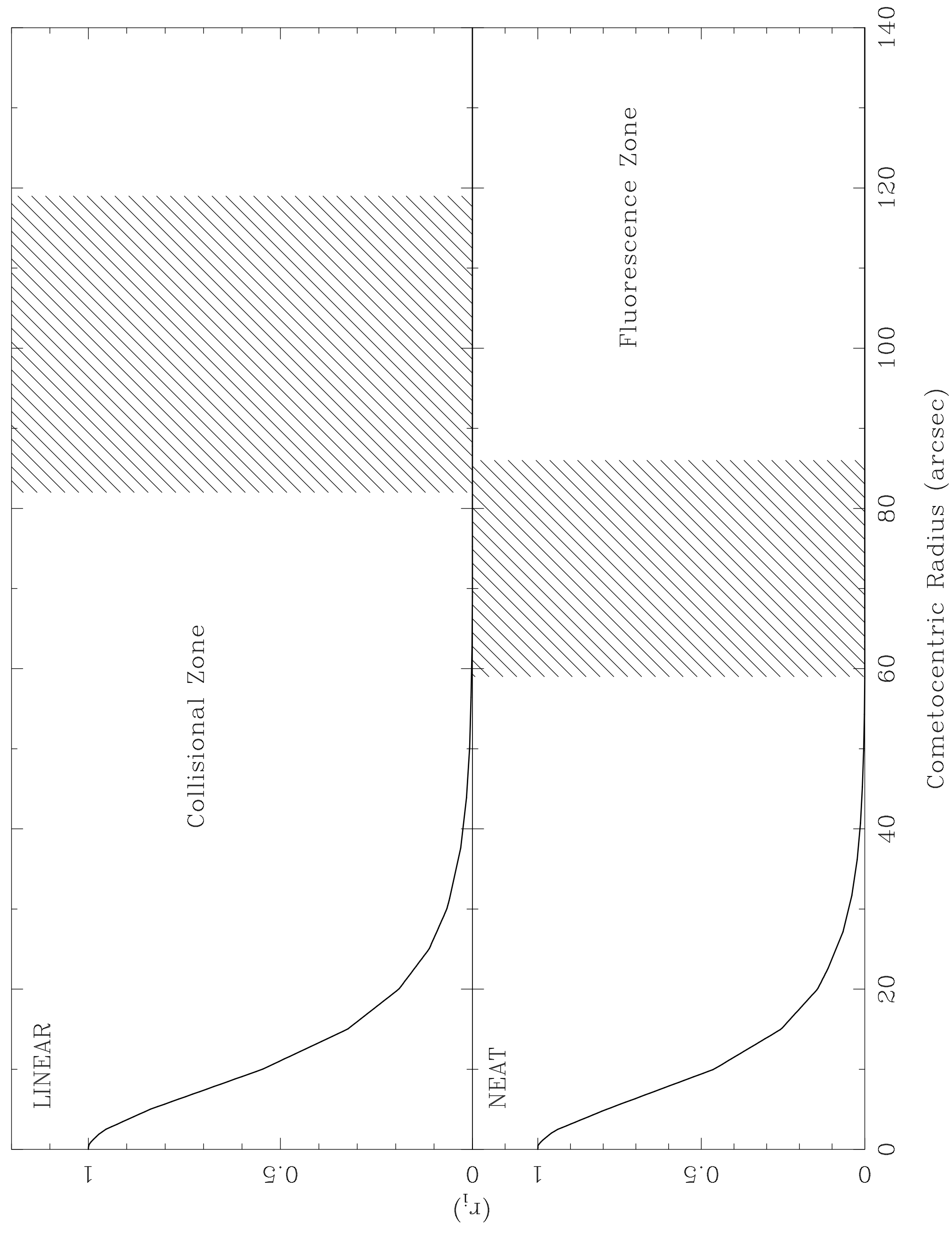
LINEAR
NEAT
Collisional Zone
Fluorescence Zone
Cometocentric Radius (arcsec)
(r_i)
0
20
40
60
80
100
120
140
0
0.5
1